Consideration and propagation of ground motion selection epistemic uncertainties to seismic performance metrics

Karim Tarbali,[a)]M.EERI, **Brendon A. Bradley,**[b),c)] M.EERI, **and Jack W. Baker**[d)] M.EERI

This paper investigates various approaches to propagate the effect of epistemic uncertainty in seismic hazard and ground motion selection to seismic performance metrics. Specifically, three approaches with different levels of rigour are presented for establishing the conditional distribution of intensity measures considered for ground motion selection, selecting ground motion ensembles, and performing nonlinear response history analyses to probabilistically characterise seismic response. The mean and distribution of the seismic demand hazard is used as the principal means to compare the various results. An example application illustrates that, for seismic demand levels significantly below the collapse limit, epistemic uncertainty in seismic response resulting from ground motion selection can generally be considered as small relative to the uncertainty in the seismic hazard itself. In contrast, uncertainty resulting from ground motion selection appreciably increases the uncertainty in the seismic demand hazard for near-collapse demand levels.

INTRODUCTION

Uncertainty in the seismic performance of engineered systems is conventionally addressed by separating uncertainty rooted from a lack of knowledge, known as 'epistemic uncertainty', from that due to apparent variability in the natural processes according to the considered mathematical model, known as 'apparent aleatory variability' (Marzocchi and Jordan, 2014). Epistemic uncertainty in the modelled characteristics of causative rupture scenarios, resulting ground motions, and the seismic response of the engineered system of interest are important steps in addressing uncertainty in seismic performance. Time-domain response history analyses (RHAs) are usually conducted to estimate the distribution of engineering demand parameters

[a)]Postdoctoral Fellow, University of Canterbury, Christchurch, New Zealand; karim.tarbali@canterbury.ac.nz
[b)]Professor, University of Canterbury, Christchurch, New Zealand
[c)]Visiting Professor, Stanford University, Stanford, CA, USA
[d)]Associate Professor, Stanford University, Stanford, CA, USA

characterising the seismic demand of the system. Conducting RHAs requires an appropriate representation of the seismic hazard at the site, which can be achieved by selecting ground motion time series recorded during past earthquakes and/or from an ensemble of simulated ground motions. While various methods have been proposed to select ground motions for seismic response analysis (*e.g.,* McGuire, 1995; Shome et al., 1998; Bommer and Acevedo, 2004; Kottke and Rathje, 2008; Baker, 2011; Jayaram et al., 2011; Wang, 2011; Bradley, 2012b) and address epistemic uncertainty in seismic hazard (*e.g.,* Kulkarni et al., 1984; Abrahamson and Bommer, 2005; McGuire et al., 2005; Bommer et al., 2005; Musson, 2005; Cotton et al., 2006; Bommer and Scherbaum, 2008; Bradley, 2009; Bommer et al., 2010; Atkinson et al., 2014; Douglas et al., 2014), the only past study concerned with the explicit consideration of seismic hazard epistemic uncertainty in the selection of ground motions is by Lin et al. (2013), which focused on epistemic uncertainty in empirical ground motion models (GMMs) and the subsequent computation of conditional pseudo spectral acceleration as the target for the ground motion selection process.

In the present study, we extend beyond Lin et al. (2013) to propagate epistemic uncertainty in both earthquake rupture forecast (ERF) and GMM aspects of probabilistic seismic hazard analysis (PSHA) to the conditional distribution of multiple intensity measures, $\boldsymbol{IM}$, utilised in ground motion selection. Different ground motion ensembles are then selected based on the epistemic uncertainty in $\boldsymbol{IM}$ to represent the seismic hazard epistemic uncertainty. Three different approaches are presented to propagate epistemic uncertainty in seismic hazard analysis and consequent ground motion selection to seismic performance measures, specifically the mean and distribution of the seismic demand hazard.

In the next sections, the main components of the seismic performance assessment procedure, and three approaches to propagate epistemic uncertainty are presented, as well as an example application to illustrate the pertinent implications.

SEISMIC PERFORMANCE ASSESSMENT PROCEDURE

The PEER framework formula considers four calculation stages to assess the seismic performance of engineered systems, including seismic hazard, response, damage, and loss assessment (Deierlein et al., 2003). Epistemic uncertainty in the performance of a system can originate from the modelling assumptions utilised at each one of these four stages. This study focuses on the consideration of, and methods to propagate, epistemic uncertainties from seismic hazard analysis and ground motion selection results to demand-based seismic performance measures by calculating the seismic demand hazard of the system (*i.e.,* probability of exceeding a seismic demand metric). That is, we exclude discussion of epistemic uncertainty in damage and loss assessment calculations, for which the reader is referred elsewhere (Taghavi and Miranda, 2003; Aslani and Miranda, 2005; Bradley, 2010a).

Computation of demand-based seismic performance measures, such as the seismic demand hazard, entails four key steps as explained in the following subsections. In this section we suppress the notational conditioning on the adopted GMM and ERF (*i.e.,* sources of seismic hazard epistemic uncertainties) which are presented in the following section explicitly based on three alternative approaches for epistemic uncertainty propagation.

STEP 1: SEISMIC HAZARD ANALYSIS

PSHA quantifies the annual exceedance frequency[a)] of a ground motion IM considering the characteristics of all causative rupture scenarios in the vicinity of the site based on an ERF as presented in Equation 1:

$$\lambda_{IM}(im) = \sum_{n=1}^{N_{rup}} P_{IM|Rup}(IM > im|rup_n)\ \lambda_{Rup}(rup_n) \tag{1}$$

where $P_{IM|Rup}(IM > im|rup_n)$ is the probability of $IM > im$ given a scenario rupture (rup_n), and $\lambda_{Rup}(rup_n)$ is the annual frequency of rup_n. As presented in Equation 1, the PSHA formulation takes into account apparent aleatory variability in the occurrence of rupture scenarios and the corresponding ground motions. Although not explicitly denoted here, the hazard curve defined via Equation 1 is conditioned on the adopted GMM and ERF, which will be later generalised for the case of multiple models representing epistemic uncertainty.

STEP 2: GROUND MOTION SELECTION

Selecting ground motion ensembles consistent with seismic hazard analysis provides the connection between seismic hazard and seismic response analyses. The severity of a ground motion is, in general, a function of amplitude, frequency content, duration, and cumulative effects. Therefore, it is pertinent to consider multiple ground motion IMs in order to take into account the salient characteristics of ground motion to accurately obtain the seismic demand distribution for the system of interest (Kramer, 1996; Bommer et al., 2004; Hancock and Bommer, 2005;

[a)] Note that the seismic hazard can be defined based on the probability of exceedance (Field et al., 2003), which enables the time-dependent seismic hazard analysis utilised for the example application in this paper.

Villaverde, 2007; Bradley, 2010b; Tarbali and Bradley, 2015b; Chandramohan et al., 2016). Since the seismic hazard is the aggregation of the threat from all seismic sources, it is also necessary to consider all causal ruptures when calculating the conditional distribution of IMs. Among several proposed methods for ground motion selection (*e.g.,* McGuire, 1995; Shome et al., 1998; Bommer and Acevedo, 2004; Kottke and Rathje, 2008; Baker, 2011; Jayaram et al., 2011; Wang, 2011; Bradley, 2012b), the generalised conditional intensity measure (GCIM) approach (Bradley, 2010b, 2012b), as the extension of the conditional mean spectrum (CMS) (Baker and Cornell, 2006; Baker, 2011), provides the required framework to address the abovementioned points. Implementing the GCIM methodology requires deaggregating the seismic hazard curve and calculating the conditional distribution of IMs considered in the ground motion selection process (as elaborated on subsequently).

Deaggregating the seismic hazard curve

Establishing the conditional distribution of various IMs requires deaggregating the seismic hazard curve to obtain the contribution of causative ruptures at a given IM level, referred to as the 'conditioning IM' (and denoted as IM_j). The contribution of a given rupture (rup_n) to the occurrence of an IM value (denoted as $IM_j = im_j$) is known as the 'occurrence' deaggregation contribution (as opposed to the exceedance deaggregation representing the contribution of scenarios to $IM_j > im_j$), and is calculated using Equation 2 (McGuire, 1995; Bazzurro and Cornell, 1999; Fox et al., 2015)[b]:

$$\begin{aligned} P_{Rup|IM_j}\left(rup_n|IM_j = im_j\right) \approx [&P_{Rup|IM_j}\left(rup_n\middle|IM_j > im_j\right)\lambda_{IM}\left(IM_j > im_j\right) - \\ &P_{Rup|IM_j}\left(rup_n|IM_j > im_j + \delta im_j\right)\lambda_{IM}\left(IM_j > im_j + \delta im_j\right)]/ \\ &[\lambda_{IM}\left(IM_j > im_j\right) - \lambda_{IM}\left(IM_j > im_j + \delta im_j\right)] \end{aligned} \tag{2}$$

where $\lambda_{IM}\left(IM_j > im_j\right)$ and $\lambda_{IM}\left(IM_j > im_j + \delta im_j\right)$ are the annual exceedance frequencies corresponding to im_j and $im_j + \delta im_j$ values obtained from the seismic hazard curve, respectively; and $P_{Rup|IM_j}\left(rup_n\middle|IM_j > im_j\right)$ is the contribution of rup_n to the exceedance of IM_j at im_j level, calculated using Equation 3:

$$P_{Rup|IM_j}\left(rup_n\middle|IM_j > im_j\right) = \frac{P_{IM_j|Rup}(IM_j > im_j|rup_n)\,\lambda_{Rup}\left(rup_n\right)}{\lambda_{IM}\left(IM_j > im_j\right)} \tag{3}$$

where $P_{IM_j|Rup}(IM_j > im_j|rup_n)$ is the exceedance probability for im_j value given rup_n obtained from the implemented GMM, $\lambda_{Rup}\left(rup_n\right)$ is the annual frequency of rup_n from the ERF, and

[b] Note that Equation 2 becomes exact in the limit as $\delta im \to 0$.

$\lambda_{IM}\left(IM_j > im_j\right)$ is the annual exceedance frequency of im_j from the seismic hazard curve.

Conditional distribution of IMs considered in ground motion selection

The target for ground motion selection in the GCIM methodology is the conditional multivariate distribution of the considered vector of IMs, $\boldsymbol{IM} = \{IM_1, IM_2, \ldots, IM_i, \ldots\}$, which accounts for various aspects of ground motion severity. The marginal conditional distribution of a single IM_i in the $\boldsymbol{IM}$ vector is obtained based on Equation 4 (Bradley, 2010b), considering the contribution of all causal ruptures to the seismic hazard at the conditioning IM level ($IM_j = im_j$):

$$f_{IM_i|IM_j}\left(im_i|im_j\right) = \sum_{n=1}^{N_{rup}} f_{IM_i|Rup,IM_j}(im_i|rup_n, im_j)\, P_{Rup|IM_j}(rup_n|IM_j = im_j) \tag{4}$$

where $f_{IM_i|Rup,IM_j}(im_i|rup_n, im_j)$ is the marginal distribution of IM_i from a single scenario rupture, rup_n, conditioned on the IM_j level considered for deaggregating the seismic hazard curve; $P_{Rup|IM_j}(rup_n|IM_j = im_j)$ is the contribution of rup_n to the occurrence of $IM_j = im_j$ obtained from Equation 2; and N_{rup} is the number of ruptures considered in the vicinity of the site. The obtained marginal IM_i distributions are used to generate realisations of the multivariate $\boldsymbol{IM}$ distribution considering the correlation between the considered IMs (see Bradley (2012b) for further details), which are then used to assess the appropriateness of the candidate ground motions (as elaborated on in the next subsection).

Selecting ground motions

In order to select an ensemble of N_{gm} ground motions, a database of prospective (recorded and/or simulated) ground motions is searched to find ground motions that fit the generated realisations of the $\boldsymbol{IM}$ distribution (Jayaram et al., 2011; Bradley, 2012b; Wang, 2011; Baker and Lee, 2017). A so-called weight vector, w_i, is used to prescribe the relative importance of the considered IM_i and calculate the misfit of each prospective ground motion with respect to the target distribution (Bradley, 2012b; Tarbali and Bradley, 2015b). Bounds on causal parameters (*e.g.,* magnitude, source-to-site distance, site condition) of prospective ground motions can also be considered prior to conducting IM-based ground motion selection (see Tarbali and Bradley (2016) and references therein).

STEP 3: SEISMIC RESPONSE ANALYSIS

Ground motion ensembles selected at different IM_j levels can be utilised to conduct RHAs of the system to calculate the distributions of engineering demand parameters (EDPs) pertinent to characterise the behaviour of the system (Jalayer and Cornell, 2009). This requires separating the results of ground motions causing collapse in the response history analysis from those resulting in non-collapse responses (Shome and Cornell, 1999). A collapse fragility function, characterising the probability of collapse for a given IM_j value, $P_{C|IM_j}\left(im_j\right)$, is established based on the proportion of ground motions resulting in collapse within the ensemble of selected records. Baker (2015) presents a maximum likelihood approach that can be used to fit a collapse fragility function to the collapse responses. Finally, when RHAs are performed for a discrete set of IM_j levels for which ground motions have been selected, interpolation is needed to develop the EDP-IM relationship. Here, linear relationships are used for $ln(EDP)$ and $\sigma_{ln(EDP)}$ with $ln(IM_j)$ to establish non-collapse response distributions (Bradley, 2013c).

The exceedance probability for the EDP of interest conditioned on an IM_j value is then obtained from Equation 5 (Shome and Cornell, 1999):

$$G_{EDP|IM_j}\left(edp|im_j\right) = G_{EDP|IM_j,NC}\left(edp|im_j\right)\left(1 - P_{C|IM_j}\left(im_j\right)\right) + P_{C|IM_j}\left(im_j\right) \tag{5}$$

where $G_{EDP|IM_j,NC}\left(edp|im_j\right)$ is the probability of $EDP > edp$ given $IM_j = im_j$ calculated from the non-collapse (NC) responses; and $P_{C|IM_j}\left(im_j\right)$ is the probability of collapse given $IM_j = im_j$ (based on the established collapse fragility function).

STEP 4: SEISMIC DEMAND HAZARD

The seismic demand hazard is calculated from (Shome and Cornell, 1999; Krawinkler and Miranda, 2004):

$$\lambda_{EDP}\left(edp\right) = \int_0^\infty G_{EDP|IM_j}\left(edp\middle|im_j\right)\left|\frac{\mathrm{d}\lambda_{IM_j}\left(im_j\right)}{\mathrm{d}IM_j}\right|\mathrm{d}IM_j \tag{6}$$

where $\mathrm{d}\lambda_{IM}\left(im_j\right)/\mathrm{d}IM_j$ is the derivative of the considered seismic hazard curve with respect to IM_j; and $G_{EDP|IM_j}\left(edp\middle|im_j\right)$ is the seismic response exceedance probability obtained from Equation 5.

Note that the distribution of EDPs of interest conditioned on a single IM_j value are conventionally utilised in seismic design guidelines (*e.g.,* NZS1170.5, 2004; ASCE/SEI7-10, 2010) to characterise the seismic performance. However, this approach neglects the fact that: (i) a certain EDP level can be exceeded at different IM_j levels; and (ii) the EDP distribution is a function of the considered IM_j (i.e., hazard) level (Bradley, 2013a). The use of the seismic demand hazard overcomes these shortcomings by taking into account the likelihood of different IM_j levels and the distribution of EDPs (conditioned on a given IM_j level), providing a more robust approach to assess the demand-based seismic performance of the system (Bradley, 2012c, 2013a).

PROPAGATION OF EPISTEMIC UNCERTAINTY

Epistemic uncertainty in the PSHA results is conventionally addressed by considering alternative GMMs and ERFs using the logic tree method[c)] (Kulkarni et al., 1984; Reiter, 1991; Bommer et al., 2005), which results in alternative plausible seismic hazard curves for the site of interest. The effect of seismic hazard epistemic uncertainty can be reflected in seismic demand measures by considering the full distribution of seismic hazard, or a single representative such as the mean or certain percentiles of the alternative hazard curves (Abrahamson and Bommer, 2005; McGuire et al., 2005; Musson, 2005). Table 1 compares the three approaches presented in the next section for propagation of seismic hazard and ground motion selection epistemic uncertainties based on the four-step demand-based seismic performance assessment procedure outlined in the previous section. As presented in Table 1, the specifics of the ground motion selection and response analysis steps, which constitute the computationally demanding steps of the process, depend on how the seismic hazard epistemic uncertainty is addressed (*i.e.,* via the full distribution of seismic hazard or simply the mean hazard). Note that Approach 2 and 3 aim to approximate the distribution and the mean demand measures from Approach 1 (*i.e.,* the exact approach). The main components of these approaches are presented in the following sections. As elaborated upon in the discussion section, since attention in this paper is focused on epistemic uncertainties in ground motion selection, then epistemic uncertainty in the seismic response of the considered engineered system is omitted, however it should be considered in practical applications.

APPROACH ONE: EXACT APPROACH

In the exact approach, each seismic hazard curve from the logic tree branches is treated separately as one possible answer to ‘what is the true seismic hazard at the site?’. Therefore, the selected ground motion ensembles, corresponding RHAs, EDP distributions, and demand hazard curve are obtained specifically for each alternative seismic hazard curve. This process results in N_{models} demand hazard curves, where N_{models} is the number of models considered to represent epistemic uncertainties in the seismic hazard.

Establishing the target distribution of IMs specific to the k^{th} logic tree branch of the seismic

[c)] The discussions to follow are equally applicable if Monte Carlo simulation is used to sample seismic hazard epistemic uncertainties.

Table 1. Comparison of three approaches to propagate the effect of epistemic uncertainties in seismic hazard analysis and ground motion selection to demand-based seismic performance measures

Step	**Approach 1: Exact**	**Approach 2:Approximate full distribution**	**Approach 3: Approximate mean**
1. Seismic hazard analysis	Complete seismic hazard distribution (all logic tree branches)		Mean hazard
2. Ground motion selection	A different GM set for every logic tree branch	One GM set corresponding to the mean hazard	
3. Seismic response analysis	Different seismic response analyses for each GM set	One set of seismic response analyses corresponding to the one GM set	
4. Seismic demand hazard	Exact distribution of the seismic demand hazard	Approximate distribution of the seismic demand hazard	Approximate mean seismic demand hazard

hazard curve requires deaggregating them at the considered conditioning IM levels. In order to have a consistent basis to establish the conditional distribution of IMs and EDP-IM relationships representing the alternative hazard curves, and compare them with those representing the mean hazard (utilised in the two approximate approaches elaborated upon subsequently), all the seismic hazard curves are deaggregated at the same conditioning IM levels. Although not strictly necessary, these IM levels may correspond to certain exceedance probabilities of the mean hazard (see Figure 1 for schematic illustration). Equations 2 and 3 are utilised for deaggregating the hazard curves for each logic tree branch resulting in the contribution of causative rupture scenario to the occurrence of $IM_j = im_j$ conditioned on the k^{th} model characteristics, *i.e.,* $P^k_{Rup|IM_j}\left(rup_n \middle| im_j\right)$.

The marginal conditional distribution of IM_i pertaining to the k^{th} model ($f^k_{IM_i|IM_j}\left(im_i \middle| im_j\right)$) is calculated based on Equation 4. Ground motion ensembles are then selected to represent the k^{th} seismic hazard curve. By conducting RHAs of the system subjected to the selected ground motions, the EDP-IM relationship specific to the k^{th} model is obtained using Equation 5. The obtained relationship is conditioned on the selected ground motion ensembles, which are themselves conditioned on the choice of GMM and ERF for the k^{th} model. The seismic demand hazard specific to the k^{th} model (*i.e.,* $\lambda^k_{EDP}(edp)$) is then calculated using Equation 6. It is emphasised that this 'exact' approach requires the selection of N_{models} different ground motion ensembles as well as performing RHAs for each and every one of these ensembles, and is therefore very computationally demanding (often prohibitively so).

The distribution of the resulting seismic demand hazard at a given EDP level, in the form of

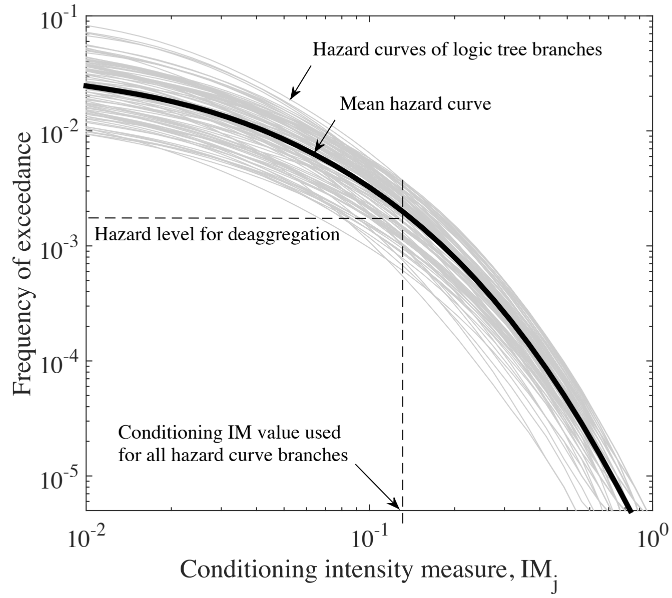

Figure 1. Schematic illustration of deaggregating the seismic hazard curve branches to establish the conditional IM distributions for ground motion selection.

cumulative probability function, is obtained using Equation 7:

$$F_{\lambda_{EDP}}[l|edp] = \sum_{k=1}^{N_{models}} I(\lambda_{EDP}^{k}(edp) \geq l)\, W_k \tag{7}$$

where $I(\lambda_{EDP}^{k}(edp) \geq l)$ is the indicator function taking the value of one for the k^{th} hazard curve resulting in a demand hazard exceedance frequency larger than or equal to l and zero otherwise; and W_k is the epistemic uncertainty weight of the k^{th} model, normalised such that $\sum_{k=1}^{N_{models}} W_k = 1$. Assuming that the considered models represent a robust set of applicable models to characterise the seismic hazard at the site, the resulting demand hazard from this exact approach can be assumed to represent the centre, body, and range in epistemic uncertainty of the seismic performance of the system due to seismic hazard and ground motion selection epistemic uncertainties.

APPROACH TWO: APPROXIMATE FULL DISTRIBUTION

Considering the significant computational burden of selecting multiple ground motion ensembles and performing RHAs of the system for every branch of the seismic hazard logic tree in the exact approach, a simplification can be applied by considering only a single EDP-IM relationship. This single EDP-IM relationship is derived based on the response of the system when subjected to ground motions representative of the mean seismic hazard. This single EDP-IM relationship can then be integrated with the alternative branches of the seismic hazard, resulting in the N_{models} demand hazard curves which tend to approximate the demand hazard distributions from the exact approach. The assumption of this approach is that the uncertainty in the EDP-IM relationship, as a result of uncertainty in the selected ground motion ensembles, is small relative to the uncertainty in the seismic hazard itself. As elaborated upon via example in Section 4.2, ground motion ensembles selected to represent the mean hazard may also be appropriate to represent the target IM distributions of logic tree branches. Hence, they can be utilised as a surrogate for branch-specific ground motion ensembles to obtain an approximation for the EDP-IM relationship. Note that Lin et al. (2013) also recommend selecting ground motion ensembles representing a single target (*i.e.,* mean hazard or variants of it); however, its integration with the mean or branches of the hazard curve logic tree was not directly discussed.

This approximate approach requires calculating the mean seismic hazard, $\overline{\lambda_{IM}}\left(im_j\right)$, which is given by:

$$\overline{\lambda_{IM_j}}\left(im_j\right) = \sum_{k=1}^{N_{models}} \lambda_{IM_j}^{k}\left(im_j\right) W_k \tag{8}$$

where $\lambda_{IM_j}^{k}\left(im_j\right)$ is the seismic hazard curve pertaining to the k^{th} logic tree branch with the corresponding weight of W_k. Note that the calculation of the mean hazard is for a specific $IM_j = im_j$ value, *i.e.,* it is a mean annual exceedance frequency, and the notion of a mean IM value for a given exceedance frequency does not have a methodological meaning (Bommer and Scherbaum, 2008).

Deaggregating the mean hazard

In order to establish the conditional distribution of IMs (considered for ground motion selection), the mean hazard curve is deaggregated with respect the contributing alternative models. The contribution of the k^{th} model to the mean hazard at a given IM level, $P_{model}^{k}\left(im_j|\overline{\lambda_{IM_j}}\left(im_j\right)\right)$, is calculated using Equation 9:

$$P_{model}^{k}\left(im_j|\overline{\lambda_{IM_j}}\left(im_j\right)\right) = \frac{\lambda_{IM_j}^{k}\left(im_j\right) W_k}{\overline{\lambda_{IM_j}}\left(im_j\right)} \tag{9}$$

The model weight in Equation 9, W_k, can be considered as the prior probability in the Bayesian statistics context, with $P_{model}^{k}\left(im_j|\overline{\lambda_{IM_j}}\left(im_j\right)\right)$ as the posterior probability obtained based on the likelihood function of $\lambda_{IM_j}^{k}\left(im_j\right)/\overline{\lambda_{IM_j}}\left(im_j\right)$. The IM distributions representing the mean hazard can be calculated based on this posterior probability (as elaborated upon in Equation 12).

The contribution of causative rupture scenarios at the conditioning IM level, $IM_j = im_j$, to the mean hazard, $\overline{P_{Rup|IM_j}}(rup_n|IM_j = im_j)$, is then calculated based on Equation 10:

$$\overline{P_{Rup|IM_j}}(rup_n|IM_j = im_j) = \sum_{k=1}^{N_{models}} P^k_{Rup|IM_j}\left(rup_n \middle| IM_j = im_j\right) P^k_{model}\left(im_j|\overline{\lambda_{IM_j}}\left(im_j\right)\right) \quad (10)$$

where $P^k_{Rup|IM_j}\left(rup_n \middle| IM_j = im_j\right)$ is the contribution of a given scenario rupture (rup_n) to the k^{th} hazard curve obtained based on Equations 2 and 3.

Conditional distribution of IMs in the approximate approach

Following Equation 4, the conditional distribution of IMs in the approximate approach is calculated using Equation 11:

$$\overline{f_{IM_i|IM_j}}\left(im_i \middle| im_j\right) = \sum_{n=1}^{N_{rup}} f_{IM_i|Rup,IM_j}(im_i|rup_n, im_j)\overline{P_{Rup|IM_j}}(rup_n|IM_j = im_j) \quad (11)$$

where $f_{IM_i|Rup,IM_j}(im_i|rup_n, im_j)$ is the marginal distribution of IM_i from a single scenario rupture conditioned on the IM_j level, and $\overline{P_{Rup|IM_j}}$ is obtained from Equation 10.

Alternatively to Equation 11, in the case where conditional distribution of IMs are already calculated for each alternative model (as, for example, in the OpenSHA software (Field et al., 2003)), these distributions can simply be combined using Equation 12 to obtain the IM distribution representing the mean hazard:

$$\overline{f_{IM_i|IM_j}}\left(im_i \middle| im_j\right) = \sum_{n=1}^{N_{models}} f^k_{IM_i|IM_j}\left(im_i \middle| im_j\right) P^k_{model}\left(im_j|\overline{\lambda_{IM_j}}\left(im_j\right)\right) \quad (12)$$

where $f^k_{IM_i|IM_j}\left(im_i \middle| im_j\right)$ is the conditional distribution of IM_i pertaining to the k^{th} model obtained based on Equation 4. Equation 11 or 12 therefore enables the calculation of conditional IM_i distributions which provide the target for selecting ground motion ensembles representing the mean hazard curve (refer to Section 2.2.3 for further details on the ground motion selection process).

Seismic demand hazard

By conducting RHAs of the system subjected to the selected ground motion ensembles representing the mean hazard, the EDP-IM relationship specific to the mean hazard curve, $\overline{G_{EDP|IM_j}}\left(edp \middle| im_j\right)$, is obtained based on Equation 5. The uncertainty in the seismic hazard can then be propagated by integrating each logic tree seismic hazard branch with the mean hazard-based EDP-IM relationship using Equation 13:

$$\widetilde{\lambda_{EDP}^{k}}(edp) = \int_0^\infty \overline{G_{EDP|IM_j}}\left(edp\middle|im_j\right)\left|\frac{\mathrm{d}\lambda_{IM_j}^{k}\left(im_j\right)}{\mathrm{d}IM_j}\right|\mathrm{d}IM_j \tag{13}$$

where $\sim$ is used to denote the approximation of $\lambda_{EDP}^{k}(edp)$ via the use of $\overline{G_{EDP|IM_j}}$ in place of $G_{EDP|IM_j}^{k}$ in the exact approach.

The distribution of demand hazards at a given EDP level from the approximate method can be calculated in the same manner as the exact approach using Equation 8.

APPROACH THREE: APPROXIMATE MEAN

The most simplified approach to calculate the demand-based seismic performance measure when addressing epistemic uncertainties in the seismic hazard and ground motion selection is to integrate the EDP-IM relationship corresponding to the mean seismic hazard (as developed in the previous subsection) with the mean seismic hazard curve (*i.e.,* Equation 8), as shown in Equation 14:

$$\overline{\lambda_{EDP}}(edp) = \int_0^\infty \overline{G_{EDP|IM_j}}\left(edp\middle|im_j\right)\left|\frac{\mathrm{d}\overline{\lambda_{IM_j}}\left(im_j\right)}{\mathrm{d}IM_j}\right|\mathrm{d}IM_j \tag{14}$$

This approach, denoted as the ‘approximate mean approach’, results in a single demand hazard curve that aims to approximate the mean value of the demand hazard curves obtained from the exact approach. It deviates from the second approach in that individual branches of the seismic hazard are not considered.

EXAMPLE APPLICATION

The San Francisco Bay Area is chosen to conduct PSHA and demonstrate the presented methodologies to propagate the effect of epistemic uncertainties, because it is a well-studied region in terms of uncertainties associated with the ERF component of PSHA, including: time-dependent nature of characteristic ruptures, magnitude-frequency distributions, magnitude-area relationships, seismogenic thickness, seismic and aseismic slip rates, distributed seismicity, fault segmentation, among others (WGCEP02, 2003). PSHA was conducted using the open-source seismic hazard analysis software OpenSHA (Field et al., 2003). Epistemic uncertainty in the ERF was considered using 100 logic tree branches of WGCEP02 (and thus each and every ERF branch has a weight of 1/100). Note that since WGCEP02 ERF is a time-dependent model, the results presented for the example application are based on exceedance probability rather than exceedance frequency[d].

Four empirical ground motion models for pseudo spectral acceleration (SA) developed as part of the next generation attenuation (NGA) project were considered in the PSHA and calculating conditional IM distributions, namely, Boore and Atkinson (2008); Chiou and Youngs (2008); Campbell and Bozorgnia (2008) and Abrahamson and Silva (2008) (referred to as BA08, CY08, CB08, and AS08, respectively). Each model is given an equal weight of 1/4 hence, in total, there exist 400 logic tree branches considering the ERF and GMM model combinations. The selected GMMs provide sufficiently appropriate tools to demonstrate the purpose of this paper.

PSHA RESULTS

The effect of epistemic uncertainties in the considered GMM and ERF branches are first illustrated through the obtained hazard curve and the deaggregation results. Figure 2a presents the hazard curves from 400 logic tree branches corresponding to SA at T =3 s vibration period, SA(3.0), obtained for a site with a V_{s30} of 400 m/s located in San Francisco (Lat 37.7833°, Long -122.4167°). Considering the time-dependent ERF of WGCEP02, PSHAs were conducted for a 30-year time period starting from 2002. Note that all the ERF branches and the considered GMMs have equal weights (of 1/400). Figure 2a shows a large range of variation in the seismic hazard due to epistemic uncertainties in the ERF (shown in grey) and GMM (shown in four colors). Figure 2b presents the contribution of the considered four GMMs to the mean hazard (*i.e.,* GMM deaggregation) calculated using Equation 9. Figure 2b shows large differences in the contribution of the considered GMMs to the mean hazard from the prior equal weight of 0.25 as the IM level increases (Lin et al., 2013).

The IM levels corresponding to 50%, 10%, 8%, 6%, 4%, 2%, 1%, 0.5%, 0.25%, 0.1%, 0.05%, 0.02% exceedance probabilities of the mean hazard curve are chosen as the conditioning IMs to deaggregate hazard curves (see Figure 1). As an illustration of variation in deaggregation results, Figure 3 presents the occurrence deaggregation contribution of the causative rupture scenarios to the conditioning IM level corresponding to 1% exceedance probability of the mean hazard (shown in the form of cumulative distribution). As shown, there is a large variation in the deaggregation contribution from alternative ERF and GMM branches with the median magnitude and source-to-site distance having ranges of [7.2-8.1] and [10-20 km], respectively (note that

[d]Due to the incompactness of the probability-based PSHA formulation (Field et al., 2003), the three methodologies presented for epistemic uncertainty prorogation are based on exceedance frequency. If the utilized ERF is time-independent, $P = 1 - e^{(-\lambda . T_{forecast})}$ can be used to convert between probability- and frequency-based results.

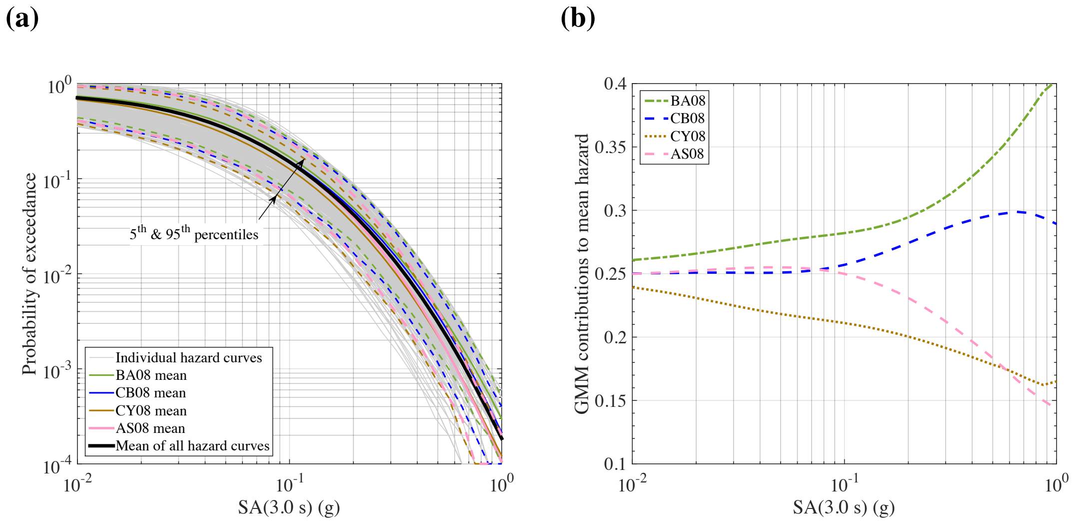

Figure 2. (a) Branch and the mean SA(3.0 s) hazard curves for a site with V_{s30}=400 m/s in San Francisco; (b) contribution of the considered GMMs to the mean hazard.

the considered site is dominated by near-source scenarios, hence a small range of variation for source-to-site distances). The variation in the deaggregation contribution of the causative rupture scenarios will propagate to the conditional distribution of IMs considered for ground motion selection and the resulting ground motion ensembles selected (as illustrated in the next section).

CONDITIONAL IM DISTRIBUTIONS AND SELECTED GROUND MOTION ENSEMBLES

The following IMs were considered in the ground motion selection process: SA ordinates for 18 vibration periods (T=0.05, 0.075, 0.1, 0.15, 0.2, 0.25, 0.3, 0.4, 0.5, 0.75, 1.0, 1.5, 2.0, 3.0, 4.0, 5.0, 7.5, and 10.0 s); cumulative absolute velocity (CAV); and 5-75% and 5-95% Significant Durations (D_{s575} and D_{s595}, respectively). These IMs represent various aspects of ground motions including amplitude, frequency content, duration, and cumulative effects, and their selection is based on other research on suitable IMs for ground motion selection (Bradley, 2012b; Tarbali and Bradley, 2015b; Chandramohan et al., 2016). The marginal distributions of SA ordinates were obtained using the corresponding GMMs utilised for the PSHA (*i.e.,* BA08, CY08, CB08, AS08). The Campbell and Bozorgnia (2010) and Kempton and Stewart (2006) GMMs were used for CAV and Significant Duration IMs, respectively. Correlations between the considered IMs were obtained based on existing empirical models (Baker and Jayaram, 2008; Bradley, 2011, 2012a). For the reasons elaborated upon subsequently in Section 5.3, epistemic uncertainties in choosing the IM correlation models and GMMs to obtain the conditional distribution of CAV, D_{s575}, and D_{s595} were not considered in this study. An ensemble of 20 ground motions was

(a) **(b)**

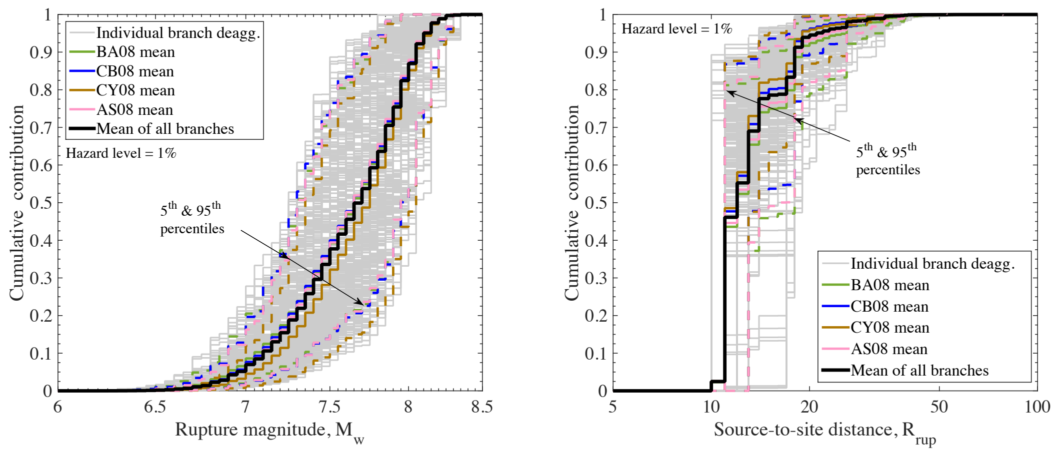

Figure 3. Cumulative contribution of causative ruptures to the IM level with 1% exceedance probability: (a) rupture magnitude; (b) source-to-site distance.

selected separately at each conditioning IM level using the GCIM methodology. A weight vector with 70% of the total weight distributed equally over the SA ordinates and 30% (equally) over CAV, D_{s575}, and D_{s595} was utilised in the ground motion selection process, which provides an appropriate weight distribution for general ground motion selection cases (Bradley, 2012b; Tarbali and Bradley, 2015b, 2016, 2015a). A subset of NGA-West2 empirical ground motion database (Ancheta et al., 2013) constrained by the causal parameter bounds recommended by Tarbali and Bradley (2016) were utilised to provide the available set of prospective records for ground motion selection.

Figure 4a presents the 16$^{\text{th}}$, 50$^{\text{th}}$, and 84$^{\text{th}}$ percentiles of the conditional SA distributions representing the SA(3.0 s) hazard at the conditioning IM level corresponding to 1% exceedance probability of the mean hazard curve. The conditional IM distributions representing the D_{s575} and CAV, and the target distributions representing the mean hazard are also presented in Figures 4c and 4e, respectively. The empirical IM_i distributions of the selected ground motion ensembles based on the IM distributions are shown in Figures 4b, d, and f. In these figures, the statistical rejections bounds based on the Kolmogorov-Smirnov (KS) test (Ang and Tang, 1975) are presented. As shown in Figures 4a, c, and e, there is a large variation in the target IM distributions due to the significant epistemic uncertainty in the PSHA results (shown in Figures 2 and 3), which are duly reflected in the properties of the selected ground motions.The selected ground motion ensembles might not in some cases properly represent the target hazard (*e.g.,* biased representation shown in Figure 4e for some of the CAV distributions as the empirical IM distributions lay outside the KS test bounds). This is due to the paucity of appropriate ground motions in the empirical database to collectively represent all the considered IMs in the selection process.

As shown in Figures 4b, d, and f, although there is a large variation, the selected ground motion ensemble corresponding to the mean hazard appears to be an appropriate ensemble to represent the target IM distributions of logic tree branches (*i.e.,* the corresponding empirical distribution lies within the KS test bounds of the target IM distributions for logic tree branches). Hence, in order to approximate the demand hazard distribution, the EDP-IM relationship obtained based on the ground motion ensembles representing the mean seismic hazard can be integrated with the seismic hazard curves from the logic tree branches (*i.e.,* the essence of the approximate full distribution approach presented previously).

RESPONSE HISTORY ANALYSIS

An inelastic single-degree-of-freedom (SDOF) system with strength and stiffness degradation (Ibarra et al., 2005; Lignos and Krawinkler, 2012), and a fundamental vibration period of T_n=3 s was subjected to the selected ground motion ensembles previously discussed. The maximum displacement of the system was chosen as the EDP of interest and the collapse limit is defined based on a nominal displacement to height ratio, specifically, 0.05, corresponding to a displacement ductility of 3.0. As noted previously, a linear relationship between ln(EDP) and ln(IM) is used to interpolate between the considered conditional IM values for the non-collapse responses (Bradley, 2013c). The maximum likelihood approach of Baker (2015) is used to establish the collapse fragility curve.

PROPAGATION OF EPISTEMIC UNCERTAINTY IN SEISMIC PERFORMANCE ASSESSMENT

Figure 5a presents the EDP-IM relationship of the SDOF system for the non-collapse responses from ground motion ensembles that are specifically selected to represent every branch of the seismic hazard curves (*i.e.,* the exact approach). The mean of the results from the exact approach and the results from the approximates approaches (for which the demand distribution is obtained based on the ground motions selected to represent the mean hazard—see Table 1), are also presented. A large variation in the EDP-IM relationship is evident especially at ground motion levels for which the response of the system is beyond the elastic response (approximately

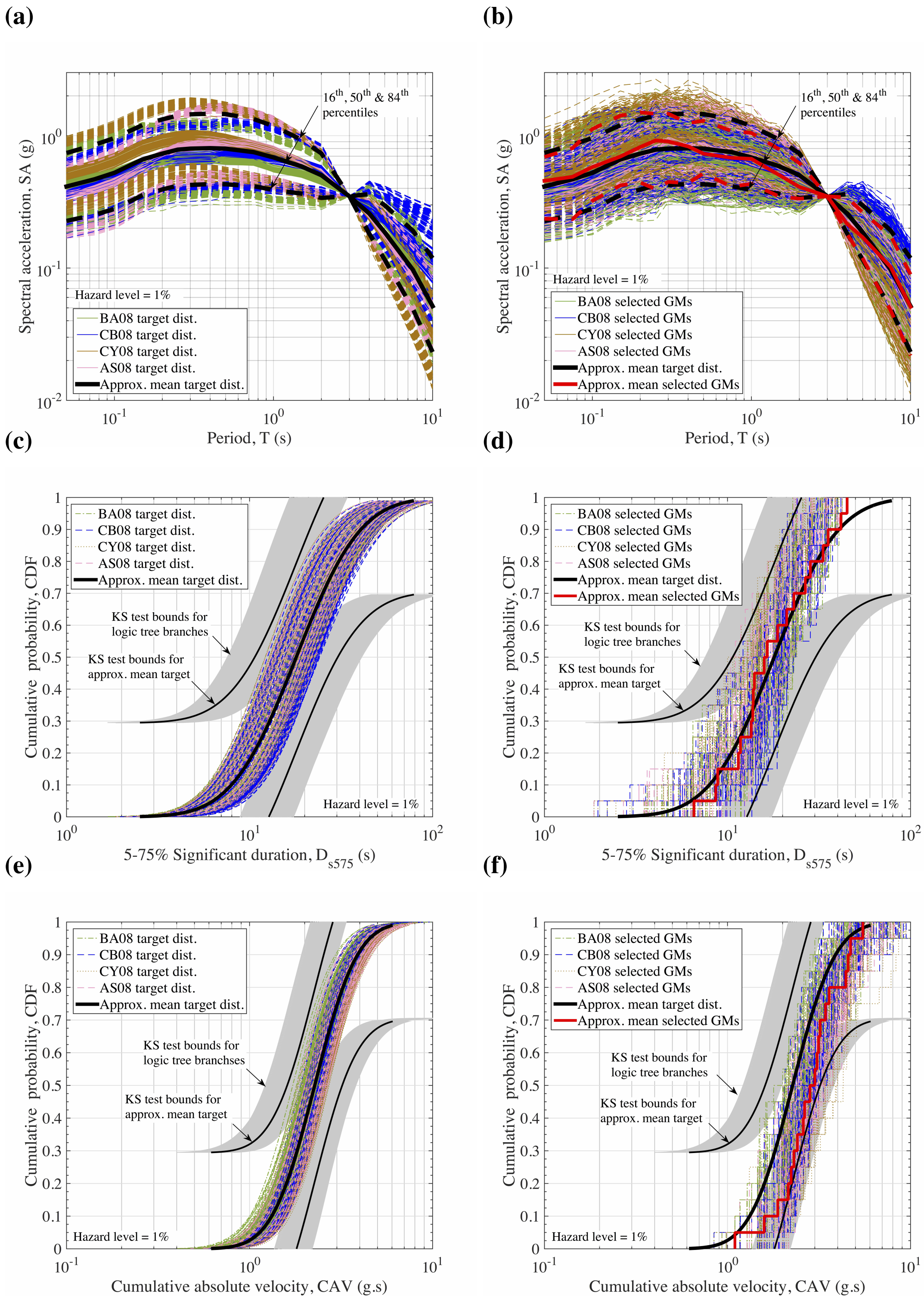

Figure 4. Conditional IM and selected ground motion distributions corresponding to the IM level with 1% exceedance probability: (a)-(b) SA ordinates; (c)-(d) Ds575; (e)-(f) CAV. The back and red lines present the target and selected ground motion distributions representing the mean seismic hazard. The coloured lines and the grey bands illustrate selected ground motion ensembles representing each and every seismic hazard branch and their corresponding KS test bounds.

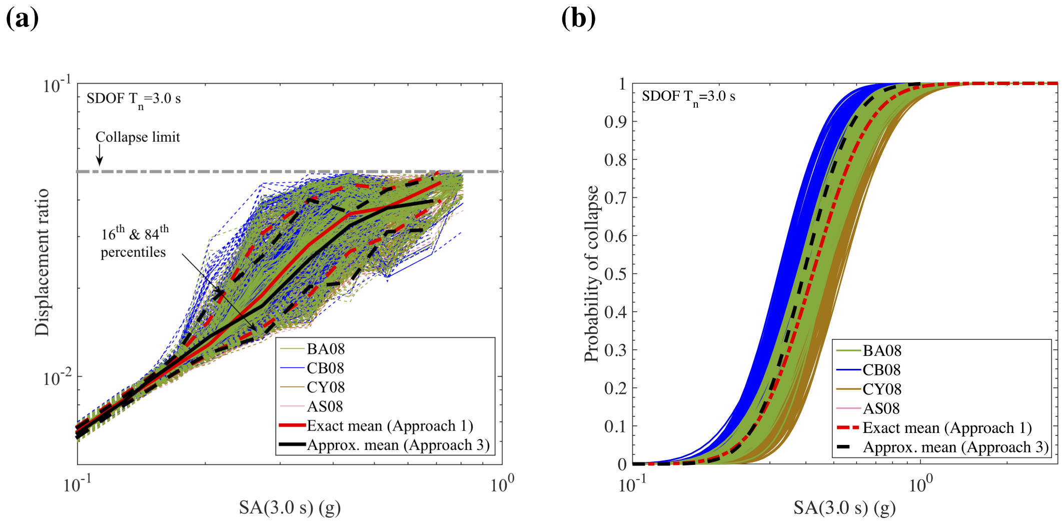

Figure 5. (a) EDP-IM relationship of the non-collapse responses; and (b) collapse fragility curves, for the T_n=3.0s SDOF system considered. The black lines illustrate the EDP and collapse probability under the mean hazard. The red lines present the mean and percentiles from the exact approach. The coloured lines illustrated the DEP and collapse probability of the system under each and every seismic hazard branch.

SA(3.0)>0.3 g). Note that the results from the approximate mean approach (shown in black), is close to the logarithmic mean from the exact approach (shown in solid red). Figure 5a also illustrates that while the 50th percentile of the non-collapse responses has an increasing trend, there might be large variations in the distribution of non-collapse responses indicated by the non-increasing trend in the 16th and 84th percentiles, due to the change in the proportion of ground motions causing collapse in the system for various IM levels.

Figure 5b presents the collapse fragility curves obtained based on the exact approach (*i.e.,* the branch-specific ground motion ensembles), separately indicated based on the GMM from the corresponding logic tree branch and their mean value, along with the results from the approximate mean approach. As shown, there is a large variation in the collapse probability for the complete IM (*i.e.,* SA(3.0 s)) range. The reason for larger approximate mean collapse probabilities from Approach 3 (for $P_{C|IM} > 0.25$) in comparison to the exact mean probabilities is the larger proportion of collapse responses (as shown in Figure 5a with a smaller median for non-collapse responses in comparison to the exact approach).

Figure 6 presents the obtained demand hazard curves from the exact (*i.e.,* Approach 1), approximate distribution (*i.e.,* Approach 2), and approximate mean (*i.e.,* Approach 3) methods, and their corresponding 1th, 16th, 50th, 84th, and 99th percentiles. As shown in Figure 6a, the exact mean demand hazard curve (from Approach 1) is appropriately estimated by the

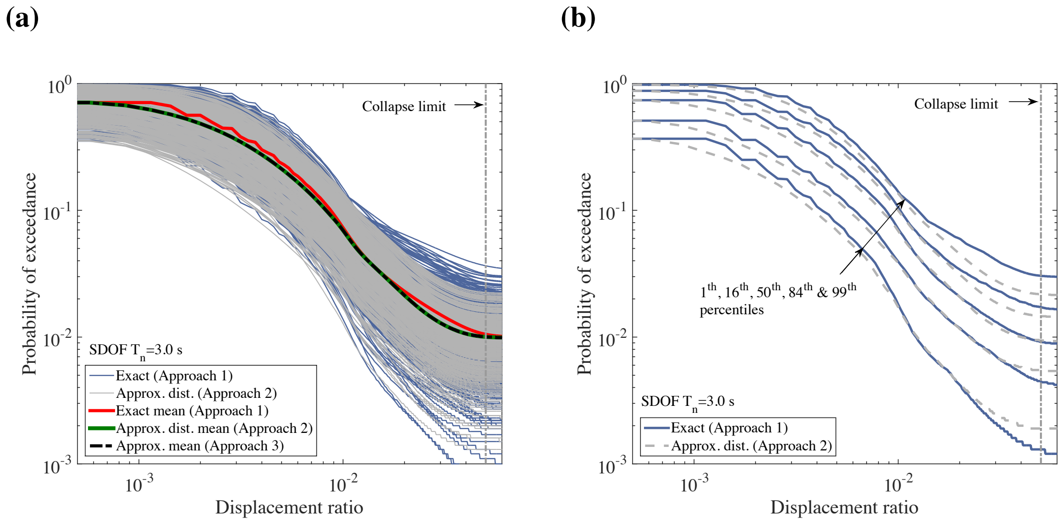

Figure 6. (a) Demand hazard curves from the three presented methodologies; (b) percentiles of the demand hazard distributions from the exact (*i.e.,* Approach 1) and approximate distribution (*i.e.,* Approach 2) methods.

approximate mean (Approach 3). Note that the mean of the results from Approach 2 (*i.e.,* the demand distribution representing the mean hazard integrated with every branch of the seismic hazard curves) is the same as that from Approach 3 (*i.e.,* the demand distribution representing the mean hazard integrated with the mean hazard). As shown in Figure 6b, while the differences between the exact and approximate distribution results are more pronounced for near-collapse EDP levels, the approximate method can appropriately estimate the demand hazard percentiles of the exact method in the whole range of EDP considered.

The presented results indicate that in cases where the objective is to obtain the mean demand hazard, it may be sufficient to integrate the mean seismic hazard with the demand distribution representing the mean hazard (*i.e.,* the approximate mean — Approach 3). Also, if the aim is to only have an approximation for the demand hazard distribution of the system, the approximate distribution (*i.e.,* Approach 2) might provide appropriate results. However, accurate assessment of epistemic uncertainties from seismic hazard and ground motion selection for demand levels near collapse likely requires the exact computation (*i.e.,* Approach 1).

DISCUSSION

COMPARISON OF DEMAND HAZARD VARIABILITY

Given the presented results, it is insightful to examine the relative contribution of: (i) seismic hazard, and (ii) ground motion selection uncertainties on the uncertainty in the seismic demand

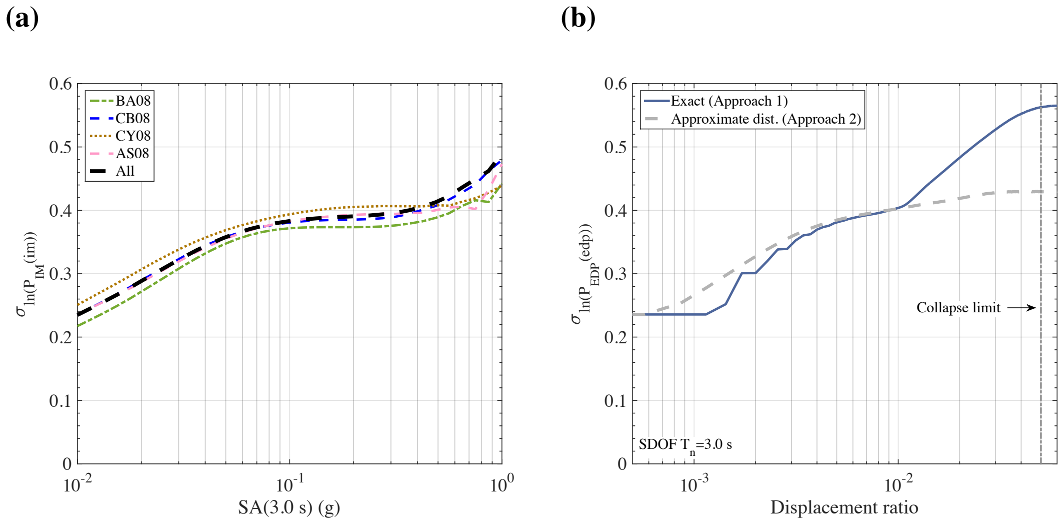

Figure 7. Dispersion of the exceedance probabilities for: (a) seismic hazard; and (b) demand hazard for the example case considered.

hazard and their dependence on the propagation approach. Figure 7a presents the lognormal standard deviation (*i.e.,* dispersion) of the seismic hazard exceedance probability, $\sigma_{ln(P_{IM}(im))}$ [e]. The results are shown for the seismic hazard curves from individual GMMs and all the seismic hazard curves combined. The dispersion of the demand hazard exceedance probability, $\sigma_{ln(P_{EDP}(edp))}$ [f], is also presented in Figure 7b. As shown, the dispersions both tend to increase with increasing IM and EDP levels, respectively. Firstly, it can be seen in Figure 7b that the dispersion in the seismic demand hazard for small EDP levels is equal to the dispersion of the seismic hazard at small IM levels. This is the result of the fact that the demand hazard for small EDPs is governed by small IMs, and that the EDP-IM relationship has small uncertainty at these IM levels (shown in Figure 5a). As the EDP level increases, the uncertainty in the EDP-IM relationship increases (due to the variability in the selected ground motion properties and increasing nonlinear response (see Figure 5a), which consequently increases the dispersion in the demand hazard. Secondly, while the demand hazard dispersion from the exact and approximate approaches is somewhat similar at small EDP levels, it is significantly different at larger (near-collapse) EDP levels.

Note that the difference between the exact and approximate approaches for estimating the dispersion in Figure 7b is simply the result of the difference in the properties of ground motions selected to represent individual logic tree branches compared to those selected to represent only the mean hazard. Because only a single ground motion ensemble is used in the approximate approaches (*i.e.,* a single EDP-IM relationship and collapse fragility curve

[e] $\sigma_{ln(\lambda_{IM}(im))}$ for frequency-based calculations
[f] $\sigma_{ln(\lambda_{EDP}(edp))}$ for frequency-based calculations

representing the response of the system under the mean hazard), uncertainty in the collapse probability distribution and EDP is not considered in the approximate approaches. In aggregate, as indicated in Figure 7b, it can be seen that ground motion selection uncertainty, leading to the EDP-IM and collapse fragility uncertainty, is significant at highly-nonlinear near-collapse seismic response levels (noting that, for example, large demand hazard dispersions of 0.56 and 0.43 in Figure 7b represent a variance ratio of 1.7 — *i.e.,* 70% increase).

COMPARISON OF THE COMPUTATIONAL BURDEN

The exact and approximate approaches for estimating the demand hazard can be compared in terms of the computational cost of propagating seismic hazard and ground motion selection epistemic uncertainties. For (i) N_{models} seismic hazard logic tree branches, (ii) deaggregated at N_{iml} IM levels, and (iii) N_{gm} ground motion selected for each ensemble; $N_{models} \times N_{iml}$ ground motion selection tasks and $N_{models} \times N_{iml} \times N_{gm}$ RHAs of the system need to be performed for the exact method. In contrast, for the approximate distribution and mean approaches these numbers are reduced to N_{iml} and $N_{iml} \times N_{gm}$, respectively (*i.e.,* a ratio of N_{models} fewer). As a typical example, considering N_{models}=100, N_{iml}=12, and N_{gm}=20, the exact approach requires 1200 ground motion selections and 24000 RHAs, whereas these numbers reduce to 12 and 240, respectively, for the two approximate approaches. Thus, given the significantly lower computational cost of the approximate approaches, it is expected that their accuracy in estimating the demand hazard will likely be deemed sufficient in many cases.

ADDITIONAL SOURCES OF EPISTEMIC UNCERTAINTY NOT CONSIDERED IN THIS STUDY

Given a GMM model utilised in seismic hazard analysis for the conditioning IM, the GMM implemented to obtain the conditional distribution of IM_i (considered in ground motion selection) can also be chosen from a set of existing models, which results in an additional level of epistemic uncertainty to consider. Note that while there is a relatively large number of GMMs to obtain SA ordinates (Douglas, 2017; Stewart et al., 2015), there is a limited number of GMMs available for other IMs, which may prevent the analyst from an appropriate representation of this additional epistemic uncertainty (Cotton et al., 2006; Bommer et al., 2010; Atkinson et al., 2014).

In addition to the epistemic uncertainty in the adopted GMMs for the considered IMs, various correlation models can be utilised in calculating the multivariate distribution of IMs considered in the ground motion selection process. In contrast to the significant differences in the IM mean and standard deviation from different GMMs (*e.g.,* Abrahamson et al., 2008; Douglas, 2017; Gregor et al., 2014; Stewart et al., 2015), different correlation models yield, in general, similar results (Baker and Bradley, 2017). Also, as illustrated by Baker and Bradley (2017), epistemic uncertainty due to the choice of GMMs to calculate the conditional distribution of IM (which will be utilised in the ground motion selection process) is significantly larger than the effect of variations in the correlation coefficients. While being another source of epistemic uncertainty in the process of seismic performance assessment, it is expected that a single correlation model will be sufficient for practical cases.

Although not considered in this paper, uncertainties in the modelling assumptions and the input parameters to create the numerical model of the system, in contrast to the two abovementioned uncertainties, is significantly important in addressing epistemic uncertainty in seismic performance assessment (Liel et al., 2009; Bradley, 2013b; Terzic et al., 2015; Gokkaya et al., 2016). These uncertainties can be addressed by considering them in the logic tree approach alongside the uncertainties from seismic hazard analysis and ground motion selection.

THE EFFECT OF MODEL SELECTION

Selecting appropriate GMMs that can represent the center, body, and range of ground motions from causative rupture scenarios for a specific region requires a rigorous approach (Cotton et al., 2006; Bommer et al., 2010; Atkinson et al., 2014). Given the fact that the NGA models utilised for the example application in this paper were developed based on similar ground motion databases and interactions between the developers, epistemic uncertainties obtained from a suite of GMMs with independent development processes can be higher for the site considered in this study (Atik and Youngs, 2014). It is important to note that alternative ERFs and GMMs implemented in any PSHA calculation represent the range of available models rather than the range of 'true' epistemic uncertainty for the site of interest (Abrahamson, 2006). As a result, a region that is not well-studied might falsely have a smaller epistemic uncertainty due to the lack of appropriate models. Since the example region chosen in this study is a well-studied region, it is expected that the effect of epistemic uncertainty on properties of the selected ground motions and seismic performance measures will be more severe for regions with greater uncertainties.

CONCLUSION

In this paper, three approaches are presented to propagate the effect of ground motion selection epistemic uncertainties to seismic performance metrics. These approaches differ in the level of rigor considered to propagate epistemic uncertainty to the conditional distribution of IMs utilised in ground motion selection, selected ground motion ensembles, and the number of response history analyses (RHAs) performed to obtain the distribution of engineering demand parameters (EDPs). In the exact approach, the EDP-IM relationship and demand hazard is calculated specifically for each seismic hazard curve from the logic tree. Assuming that the considered models represent a robust set of applicable models to characterise the seismic hazard at the site, the resulting demand hazards from the exact approach can be assumed to represent the centre, body, and range in epistemic uncertainty of seismic performance of the system. In contrast, an approximate distribution approach utilises the EDP-IM relationship and collapse fragility curve obtained based on ground motion ensembles representing only the mean seismic hazard curve, which is then integrated with hazard curves from the logic tree branches to obtain an approximation to the demand hazard obtained from the exact approach. This approach has a significantly lower computational cost compared to the exact approach due to the smaller number of RHAs and ground motion selection tasks performed. The third (*i.e.,* approximate mean) approach integrates the EDP-IM relationship and collapse fragility curve representing the mean hazard with the mean seismic hazard curve, resulting in a demand hazard which aims to approximate the mean from the exact approach.

The three presented approaches were compared for an example in the San Francisco Bay Area considering epistemic uncertainties in the earthquake rupture forecast and ground motion models. The presented results indicate that considering the significantly lower computational cost of utilising the approximate distribution approach, this approach can appropriately approximate the distribution of the demand hazards from the exact approach. In addition, if the aim is to obtain the mean demand hazard, it is sufficient to integrate the mean seismic hazard with the EDP-IM relationship and collapse fragility curve representing the mean seismic hazard. Also, it was observed that, for seismic demand levels below the collapse limit, epistemic uncertainty in ground motion selection is a smaller uncertainty contributor relative to the uncertainty in the seismic hazard itself. In contrast, uncertainty in ground motion selection process increases the uncertainty in the seismic demand hazard for near-collapse demand levels.

ACKNOWLEDGEMENTS

This research was partially supported by the Royal Society of New Zealand, Natural Hazards Research Platform, and QuakeCoRE: The New Zealand Centre of Earthquake Resilience. This is QuakeCoRE publication 189.

REFERENCES

Abrahamson, N., 2006. Seismic hazard assessment: problems with current practice and future developments. In *First European Conference on Earthquake Engineering and Seismology*, pp. 3–8.

Abrahamson, N., Atkinson, G., Boore, D., Bozorgnia, Y., Campbell, K., Chiou, B., Idriss, I., Silva, W., and Youngs, R., 2008. Comparisons of the NGA ground-motion relations. *Earthquake Spectra* **24**, 45–66.

Abrahamson, N. and Silva, W., 2008. Summary of the Abrahamson & Silva NGA ground-motion relations. *Earthquake spectra* **24**, 67–97.

Abrahamson, N. A. and Bommer, J. J., 2005. Probability and uncertainty in seismic hazard analysis. *Earthquake Spectra* **21**, 603–607.

Ancheta, T. D., Darragh, R., Stewart, J., Seyhan, E., Silva, W., Chiou, B., Wooddell, K., Graves, R., Kottke, A., and Boore, D., 2013. PEER NGA-West2 Database. *PEER Report 2013* **3**.

Ang, A. H. and Tang, W. H., 1975. *Probability concepts in engineering planning and design*. John Wiley & Sons, Inc., New York.

ASCE/SEI7-10, 2010. Minimum Design Loads for Buildings and Other Structures, ASCE/SEI 7-10. American Society of Civil Engineers, Reston, Virginia.

Aslani, H. and Miranda, E., 2005. Probabilistic earthquake loss estimation and loss disaggregation in buildings. Thesis.

Atik, L. A. and Youngs, R. R., 2014. Epistemic uncertainty for NGA-West2 models. *Earthquake Spectra* **30**, 1301–1318.

Atkinson, G. M., Bommer, J. J., and Abrahamson, N. A., 2014. Alternative approaches to modeling epistemic uncertainty in ground motions in probabilistic seismic-hazard analysis. *Seismological Research Letters* **85**, 1141–1144.

Baker, J. W., 2011. Conditional mean spectrum: Tool for ground-motion selection. *Journal of Structural Engineering* **137**, 322–331.

Baker, J. W., 2015. Efficient analytical fragility function fitting using dynamic structural analysis. *Earthquake Spectra* **31**, 579–599.

Baker, J. W. and Bradley, B. A., 2017. Intensity measure correlations observed in the NGA-West2 database, and dependence of correlations on rupture and site parameters. *Earthquake Spectra* **33**, 145–156.

Baker, J. W. and Cornell, A. C., 2006. Spectral shape, epsilon and record selection. *Earthquake Engineering & Structural Dynamics* **35**, 1077–1095.

Baker, J. W. and Jayaram, N., 2008. Correlation of spectral acceleration values from NGA ground motion models. *Earthquake Spectra* **24**, 299–317.

Baker, J. W. and Lee, C., 2017. An Improved Algorithm for Selecting Ground Motions to Match a

Conditional Spectrum. *Journal of Earthquake Engineering* pp. 1–16.

Bazzurro, P. and Cornell, C. A., 1999. Disaggregation of seismic hazard. *Bulletin of the Seismological Society of America* **89**, 501–520.

Bommer, J. J. and Acevedo, A. B., 2004. The use of real earthquake accelerograms as input to dynamic analysis. *Journal of Earthquake Engineering* **8**, 43–91.

Bommer, J. J., Douglas, J., Scherbaum, F., Cotton, F., Bungum, H., and Fah, D., 2010. On the selection of ground-motion prediction equations for seismic hazard analysis. *Seismological Research Letters* **81**, 783–793.

Bommer, J. J., Magenes, G., Hancock, J., and Penazzo, P., 2004. The influence of strong-motion duration on the seismic response of masonry structures. *Bulletin of Earthquake Engineering* **2**, 1–26.

Bommer, J. J. and Scherbaum, F., 2008. The use and misuse of logic trees in probabilistic seismic hazard analysis. *Earthquake Spectra* **24**, 997–1009.

Bommer, J. J., Scherbaum, F., Bungum, H., Cotton, F., Sabetta, F., and Abrahamson, N. A., 2005. On the use of logic trees for ground-motion prediction equations in seismic-hazard analysis. *Bulletin of the Seismological Society of America* **95**, 377–389.

Boore, D. M. and Atkinson, G. M., 2008. Ground-motion prediction equations for the average horizontal component of PGA, PGV, and 5and 10.0 s. *Earthquake Spectra* **24**, 99–138.

Bradley, B. A., 2009. Seismic hazard epistemic uncertainty in the San Francisco bay area and its role in performance-based assessment. *Earthquake Spectra* **25**, 733–753.

Bradley, B. A., 2010a. Epistemic uncertainties in component fragility functions. *Earthquake Spectra* **26**, 41–62.

Bradley, B. A., 2010b. A generalized conditional intensity measure approach and holistic ground-motion selection. *Earthquake Engineering & Structural Dynamics* **39**, 1321–1342.

Bradley, B. A., 2011. Correlation of significant duration with amplitude and cumulative intensity measures and its use in ground motion selection. *Journal of Earthquake Engineering* **15**, 809–832.

Bradley, B. A., 2012a. Empirical correlations between cumulative absolute velocity and amplitude-based ground motion intensity measures. *Earthquake Spectra* **28**, 37–54.

Bradley, B. A., 2012b. A ground motion selection algorithm based on the generalized conditional intensity measure approach. *Soil Dynamics and Earthquake Engineering* **40**, 48–61.

Bradley, B. A., 2012c. The seismic demand hazard and importance of the conditioning intensity measure. *Earthquake Engineering & Structural Dynamics* **41**, 1417–1437.

Bradley, B. A., 2013a. A comparison of intensity-based demand distributions and the seismic demand hazard for seismic performance assessment. *Earthquake Engineering & Structural Dynamics* **42**, 2235–2253.

Bradley, B. A., 2013b. A critical examination of seismic response uncertainty analysis in earthquake engineering. *Earthquake Engineering & Structural Dynamics* **42**, 1717–1729.

Bradley, B. A., 2013c. Practice-oriented estimation of the seismic demand hazard using ground motions at few intensity levels. *Earthquake Engineering & Structural Dynamics* **42**, 2167–2185.

Campbell, K. W. and Bozorgnia, Y., 2008. NGA ground motion model for the geometric mean horizontal component of PGA, PGV, PGD and 5ranging from 0.01 to 10 s. *Earthquake Spectra* **24**, 139–171.

Campbell, K. W. and Bozorgnia, Y., 2010. A ground motion prediction equation for the horizontal component of cumulative absolute velocity (CAV) based on the PEER-NGA strong motion database. *Earthquake Spectra* **26**, 635–650.

Chandramohan, R., Baker, J. W., and Deierlein, G. G., 2016. Impact of hazard-consistent ground motion duration in structural collapse risk assessment. *Earthquake Engineering & Structural Dynamics* .

Chiou, B.-J. and Youngs, R. R., 2008. An NGA model for the average horizontal component of peak ground motion and response spectra. *Earthquake Spectra* **24**, 173–215.

Cotton, F., Scherbaum, F., Bommer, J. J., and Bungum, H., 2006. Criteria for selecting and adjusting ground-motion models for specific target regions: Application to central Europe and rock sites. *Journal of Seismology* **10**, 137–156.

Deierlein, G., Krawinkler, H., and Cornell, C., 2003. A framework for performance-based earthquake engineering. In *Pacific conference on earthquake engineering*, pp. 1–8. Citeseer.

Douglas, J., 2017. Ground motion prediction equations 1964–2017, http://www.gmpe.org.uk.

Douglas, J., Ulrich, T., Bertil, D., and Rey, J., 2014. Comparison of the ranges of uncertainty captured in different seismic-hazard studies. *Seismological Research Letters* **85**, 977–985.

Field, E. H., Jordan, T. H., and Cornell, C. A., 2003. OpenSHA: A developing community-modeling environment for seismic hazard analysis. *Seismological Research Letters* **74**, 406–419.

Fox, M. J., Stafford, P. J., and Sullivan, T. J., 2015. Seismic hazard disaggregation in performance-based earthquake engineering: occurrence or exceedance? *Earthquake Engineering & Structural Dynamics* .

Gokkaya, B. U., Baker, J. W., and Deierlein, G. G., 2016. Quantifying the impacts of modeling uncertainties on the seismic drift demands and collapse risk of buildings with implications on seismic design checks. *Earthquake Engineering & Structural Dynamics* **45**, 1661–1683.

Gregor, N., Abrahamson, N. A., Atkinson, G. M., Boore, D. M., Bozorgnia, Y., Campbell, K. W., Chiou, B. S.-J., Idriss, I., Kamai, R., and Seyhan, E., 2014. Comparison of NGA-West2 GMPEs. *Earthquake Spectra* **30**, 1179–1197.

Hancock, J. and Bommer, J. J., 2005. The effective number of cycles of earthquake ground motion. *Earthquake engineering & structural dynamics* **34**, 637–664.

Ibarra, L. F., Medina, R. A., and Krawinkler, H., 2005. Hysteretic models that incorporate strength and stiffness deterioration. *Earthquake engineering & structural dynamics* **34**, 1489–1511.

Jalayer, F. and Cornell, C., 2009. Alternative non-linear demand estimation methods for probability-based seismic assessments. *Earthquake Engineering & Structural Dynamics* **38**, 951–972.

Jayaram, N., Lin, T., and Baker, J. W., 2011. A computationally efficient ground-motion selection algorithm for matching a target response spectrum mean and variance. *Earthquake Spectra* **27**, 797–815.

Kempton, J. J. and Stewart, J. P., 2006. Prediction equations for significant duration of earthquake ground motions considering site and near-source effects. *Earthquake spectra* **22**, 985–1013.

Kottke, A. and Rathje, E. M., 2008. A semi-automated procedure for selecting and scaling recorded earthquake motions for dynamic analysis. *Earthquake Spectra* **24**, 911–932.

Kramer, S. L., 1996. *Geotechnical earthquake engineering*. Pearson Education India. ISBN 8131707180.

Krawinkler, H. and Miranda, E., 2004. *Performance-based earthquake engineering*. CRC Press, Boca Raton, FL.

Kulkarni, R., Youngs, R., and Coppersmith, K., 1984. Assessment of confidence intervals for results of seismic hazard analysis. In *Proceedings of the Eighth World Conference on Earthquake Engineering*, vol. 1, pp. 263–270.

Liel, A. B., Haselton, C. B., Deierlein, G. G., and Baker, J. W., 2009. Incorporating modeling uncertainties in the assessment of seismic collapse risk of buildings. *Structural Safety* **31**, 197–211.

Lignos, D. G. and Krawinkler, H., 2012. Development and utilization of structural component databases for performance-based earthquake engineering. *Journal of Structural Engineering* **139**, 1382–1394.

Lin, T., Harmsen, S. C., Baker, J. W., and Luco, N., 2013. Conditional Spectrum Computation Incorporating Multiple Causal Earthquakes and Ground-Motion Prediction Models. *Bulletin of the Seismological Society of America* **103**, 1103–1116.

Marzocchi, W. and Jordan, T. H., 2014. Testing for ontological errors in probabilistic forecasting models of natural systems. *Proceedings of the National Academy of Sciences* **111**, 11973–11978.

McGuire, R. K., 1995. Probabilistic seismic hazard analysis and design earthquakes: closing the loop. *Bulletin of the Seismological Society of America* **85**, 1275–1284.

McGuire, R. K., Cornell, C. A., and Toro, G. R., 2005. The case for using mean seismic hazard. *Earthquake Spectra* **21**, 879–886.

Musson, R., 2005. Against fractiles. *Earthquake Spectra* **21**, 887–891.

NZS1170.5, 2004. NZS1170.5:2004 Structural design actions, Part 5: Earthquake actions - New Zealand.

Reiter, L., 1991. *Earthquake hazard analysis: issues and insights*. Columbia University Press. ISBN 0231513208.

Shome, N. and Cornell, C., 1999. *probabilistic seismic demand analysis of nonlinear structures*. *Report*, Stanford University: Palo Alto, CA.

Shome, N., Cornell, C. A., Bazzurro, P., and Carballo, J. E., 1998. Earthquakes, records, and nonlinear responses. *Earthquake Spectra* **14**, 469–500.

Stewart, J. P., Douglas, J., Javanbarg, M., Bozorgnia, Y., Abrahamson, N. A., Boore, D. M., Campbell, K. W., Delavaud, E., Erdik, M., and Stafford, P. J., 2015. Selection of ground motion prediction equations for the Global Earthquake Model. *Earthquake Spectra* **31**, 19–45.

Taghavi, S. and Miranda, E., 2003. *Response assessment of nonstructural building elements*. Pacific Earthquake Engineering Research Center.

Tarbali, K. and Bradley, B. A., 2015a. *Bounds on causal parameters of prospective ground motions and their effect on characteristics of selected ground motions, Department of Civil and Natural Resources Engineering, Research Report 2015-01, University of Canterbury, New Zealand, https://ir.canterbury.ac.nz/handle/10092/13314*. *Report*. doi:https://ir.canterbury.ac.nz/handle/10092/13314.

Tarbali, K. and Bradley, B. A., 2015b. Ground-motion selection for scenario ruptures using the generalized conditional intensity measure (GCIM) method. *Earthquake Engineering & Structural Dynamics* **44**, 1601–1621. doi:10.1002/eqe.2546.

Tarbali, K. and Bradley, B. A., 2016. The Effect of Causal Parameter Bounds in PSHA-based Ground Motion Selection. *Earthquake Engineering & Structural Dynamics* **45**, 1515–1535.

Terzic, V., Schoettler, M., Restrepo, J., and Mahin, S., 2015. Concrete column blind prediction contest 2010: outcomes and observations. *PEER Rep. No* **1**.

Villaverde, R., 2007. Methods to assess the seismic collapse capacity of building structures: State of the art. *Journal of Structural Engineering* **133**, 57–66.

Wang, G., 2011. A ground motion selection and modification method capturing response spectrum characteristics and variability of scenario earthquakes. *Soil Dynamics and Earthquake Engineering* **31**, 611–625.

WGCEP02, 2003. *Working Group on California Earthquake Probabilities: Earthquake probabilities in the San Francisco Bay region: 2002-2031, Open-File Report 03-214. Report.*